# Shear-Wave Velocity Studies of Near-Surface Deposits in the Fort St. John–Dawson Creek Area, Northeastern British Columbia (NTS 093P, 094A)

**P.A. Monahan,** Monahan Petroleum Consulting, Victoria, British Columbia, pmonahan@shaw.ca

**B.J. Hayes,** Petrel Robertson Consulting Ltd., Calgary, Alberta

**M. Perra,** Petrel Robertson Consulting Ltd., Calgary, Alberta

**Y. Mykula,** Petrel Robertson Consulting Ltd., Calgary, Alberta

**J. Clarke,** Petrel Robertson Consulting Ltd., Calgary, Alberta

**C. Gugins,** Frontier Geosciences Inc., North Vancouver, British Columbia

**C. Candy,** Frontier Geosciences Inc., North Vancouver, British Columbia

**D. Griffiths,** Frontier Geosciences Inc., North Vancouver, British Columbia

**O. Bayarsaikhan,** Frontier Geosciences Inc., North Vancouver, British Columbia

**O. Jones,** Frontier Geosciences Inc., North Vancouver, British Columbia

**U. Oki,** Metro Testing + Engineering Ltd., Fort St. John, British Columbia

Monahan, P.A., Hayes, B.J., Perra, M., Mykula, Y., Clarke, J., Gugins, C., Candy, C., Griffiths, D., Bayarsaikhan, O., Jones, O. and Oki, U. (2021): Shear-wave velocity studies of near-surface deposits in the Fort St. John–Dawson Creek area, northeastern British Columbia (NTS 093P, 094A); *in* Geoscience BC Summary of Activities 2020: Energy and Water, Geoscience BC, Report 2021-02, p. 1–16.

## Introduction

Seismicity in northeastern British Columbia (BC) has recently increased significantly due to hydraulic fracturing and water disposal by the petroleum industry (Atkinson et al., 2016; Kao et al., 2018; Roth, 2020). Most of these events are small, but rare events up to magnitude (M) 4.6 have occurred (Babaie Mahani et al., 2017a, b, 2019). Ground motions for the largest events are at the lower bound of possible damage, in the range of modified Mercalli intensity (MMI) VI (Worden et al., 2012; Babaie Mahani and Kao, 2018; Babaie Mahani et al., 2019).

As part of an investigation of the potential for amplification of seismic ground motions, shear-wave ($V_S$) data for near-surface geological deposits have been acquired at 28 sites in the Fort St. John–Dawson Creek area of northeastern BC. This area is in the southern part of the Montney gas play area, which is currently the most active gas play in BC and is being extensively developed by hydraulic fracturing in horizontal wells. A M4.6 induced event occurred in this area in November 2018 (Babaie Mahani et al., 2019). The objective of this paper is to summarize the results of the $V_S$ data acquisition and to present a $V_S$ model of the shallow geological deposits. Other aspects of this project are described by Monahan et al. (2020).

*This publication is also available, free of charge, as colour digital files in Adobe Acrobat® PDF format from the Geoscience BC website: http://geosciencebc.com/updates/summary-of-activities/.*

## Ground-Motion Amplification

Ground-motion amplification due to shallow geological conditions can be estimated by the time-averaged $V_S$ in the upper 30 m ($V_{S30}$, harmonic mean), with amplification susceptibility increasing as $V_{S30}$ decreases (Table 1; Kramer, 1996; Building Seismic Safety Council, 2003; Finn and Wightman, 2003; National Research Council, 2015).

Amplification can also be due to resonance in the soil column, where the dominant period of the ground motions is the same as the dominant site period. Amplification due to resonance was also suspected in the region by Monahan et al. (2019).

## Regional Geology

The project area is located in the western part of the Alberta Plateau (Holland, 1976), and extends from Fort St. John to Dawson Creek and from the Alberta border west to the Pine and Moberly rivers (Figure 1). The plateau is incised by valleys, up to 280 m deep, of the Peace River and its major tributaries, the Kiskatinaw, Pine, Moberly, Pouce Coupé and Beatton rivers. Adjacent to these valleys, low relief benches form the plateau surface, and these extend up smaller valleys into the hilly uplands that lie farther from the rivers. In the uplands in the western part of the project

**Table 1.** National Earthquake Hazards Reduction Program (NEHRP) Site classes, also adopted by the National Building Code of Canada (Building Seismic Safety Council, 2003; National Research Council, 2015). Susceptibility ratings from Hollingshead and Watts (1994).

| Site Class | General description | Definition by $V_{S30}$ | Susceptibility rating |
|---|---|---|---|
| A | Hard rock | $V_{S30}$>1500 | Nil |
| B | Rock | 760<$V_{S30}$<1500 | Very low |
| C | Very dense soils and soft rock | 360<$V_{S30}$<760 | Low |
| D | Stiff soils | 180<$V_{S30}$<360 | Moderate |
| E | Soft soils | $V_{S30}$<180 | High |

area, hilltops are up to 900 metres above sea level (m asl) in elevation and the local relief is up to 200 m. The topography of the uplands becomes more subdued toward the east, where hilltops are up to 700 m asl in elevation and local relief is 50 m.

Bedrock at surface consists of gently easterly dipping, relatively soft Cretaceous sedimentary rocks (Irish, 1958; Stott, 1982; McMechan, 1994; Plint, 2000). The principal geological units exposed from northwest to southeast across the project area are, in ascending order, the Shaftesbury Formation, which consists of marine shale; the Dunvegan Formation, which consists of marine and nonmarine sandstone, conglomerate and shale; the Kaskapau Formation, which consists of marine shale, with sandstone members in its lower part; and the Cardium Formation, which consists of marine and nonmarine sandstone, conglomerate and shale. The upper 5 to 30 m of bedrock is commonly weathered to clay, particularly the shale intervals, and the upper surface is commonly glaciotectonized (Monahan et al., 2019, 2020).

At least three glaciations occurred during the Quaternary in this area (Mathews, 1978; Hartman and Clague, 2008; Hickin et al., 2015, 2016a, b). Deposits of the last two glacial and adjoining nonglacial periods show a repetitive pattern of fluvial incision and deposition during nonglacial intervals, followed by deposition of glaciolacustrine silt as drainageways were blocked by advancing Laurentide ice, and finally, by till during the glacial maximum. Fluvial incision cut deeper following each glaciation, so that modern valleys of the Peace River and its major tributaries are incised through the older Quaternary deposits into bedrock.

Deposits of the latest glaciation, during the Late Wisconsinan, are the best known (Mathews, 1978, 1980; Hartman and Clague, 2008; Hickin et al., 2015, 2016a, b). Both Cordilleran and Laurentide ice extended into the area, but the maximum extents of each appear to have been out of sync. West of the project area, Cordilleran till has been reported interbedded with advance-phase glaciolacustrine deposits (glacial Lake Mathews; Hartman et al., 2018). However, the advance-phase glaciolacustrine deposits are overlain by clay-rich till deposited by Laurentide ice. The ice sheets appear to have coalesced, but in the latter stages, Laurentide till appears to have been overridden locally by Cordilleran ice (Hickin et al., 2016b). As Laurentide ice retreated, drainage was again blocked, resulting in widespread deposition of glaciolacustrine silt, clay and very fine sand of glacial Lake Peace. Following drainage of this lake, fluvial incision resumed and continued into the Holocene.

Sediments older than the last glacial maximum are restricted to Quaternary river valleys (paleovalleys) that underlie benches adjacent to the major rivers and some smaller valleys. They are exposed only in the valley walls of the Peace River and its tributaries. Elsewhere, only Late Wisconsinan till, retreat-phase deposits and Holocene sediments occur at the surface. These units occur in specific geomorphic settings (Mathews, 1978; Reimchen, 1980; Hartman and Clague, 2008; Hickin et al., 2015; Monahan et al., 2019). The uplands are underlain mainly by till with a veneer of glaciolacustrine silt and clay. Topography in the uplands is largely controlled by bedrock, which is locally exposed and generally within a few metres of the surface in the western parts of the project area. However, in the uplands of more subdued relief in the eastern part of the project area, till commonly forms a blanket up to 30 m thick. The low relief benches, between the uplands and deeply incised major valleys, are underlain by retreat-phase glaciolacustrine and related deposits, which are 10 to 15 m thick adjacent to the major rivers and between 5 and 50 m thick in smaller valleys. Where these deposits overlie older Pleistocene deposits in paleovalleys, the total Quaternary thickness locally exceeds 200 m. Terraces on the walls of major valleys are underlain by late stage Wisconsinan glaciofluvial sand and gravel representing the earliest phases of postglacial fluvial incision and are up to 30 m thick. Modern fluvial sand and gravel occupies river valley bottoms.

Within the upland areas, the valleys of smaller streams have gently sloping floors and are underlain by glaciolacustrine sediments, into which the modern streams have now incised. The degree of incision increases markedly as these streams approach the major valleys. Boundaries between

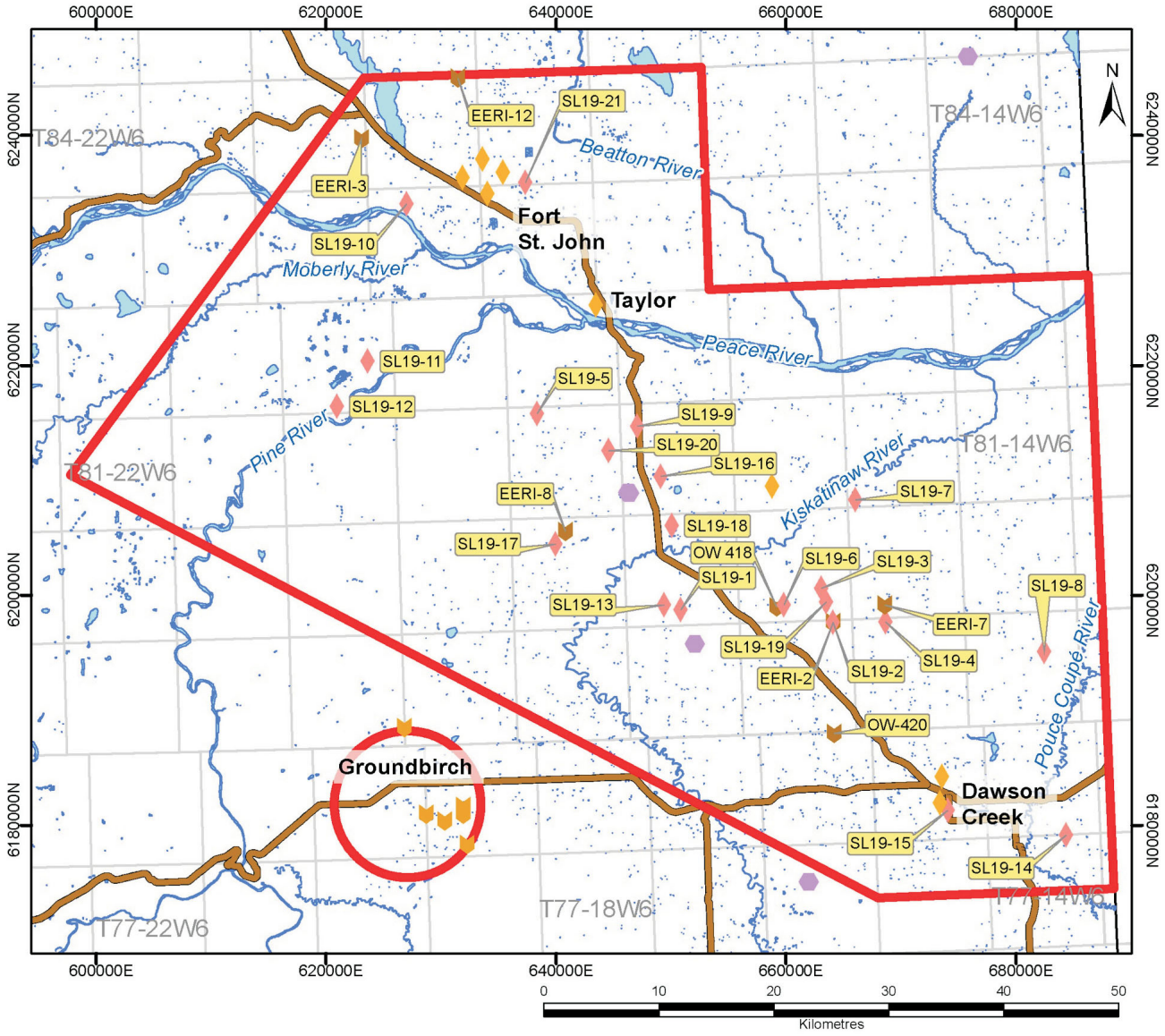


**Figure 1**. Spatial distribution of sites where shear-wave velocity ($V_S$) data were acquired in the Fort St. John–Dawson Creek area, northeastern British Columbia. Site details are found in Tables 2 and 3. The previous study noted is that by Monahan et al. (2019). Abbreviations: MASW, multichannel analysis of surface waves; VSP, vertical seismic profiling. UTM Zone 10N, NAD 83.

the upland areas and adjacent glaciolacustrine benches and valley bottoms are commonly marked by distinct breaks in slope. However, these breaks in slope are not as clear in the areas of subdued topography in the east.

## Acquisition of $V_S$ Data

Shear-wave velocity ($V_S$) data have been acquired at 28 sites, by downhole logging in existing boreholes using the vertical seismic profiling (VSP) method, and by multichannel analysis of surface waves (MASW), a non-invasive surface technique that generates a $V_S$ profile along a 100 m transect. These two methods are described by Arsenault et al. (2012) and Phillips and Sol (2012), respectively. The data were acquired by Frontier Geosciences Inc.

The VSP logs were acquired in seven boreholes, and the results are summarized in Table 2. Five of the boreholes were drilled by the Energy and Environment Research Initiative (EERI) as part of a regional groundwater monitoring project by the University of British Columbia (Cahill et al., 2019; Ladd et al., 2019, 2020), and the other two are Province of BC groundwater observation wells (OW; Kelly and Janicki, 2013). In addition to $V_S$, P-wave velocity ($V_P$) data were obtained at all sites, and gamma-ray logs were run in EERI-2, and -3, and OW 418 and 420 to correlate with gamma-ray logs in nearby petroleum wells. The EERI boreholes have polyvinyl chloride (PVC) casing, whereas the OW have steel casing to the approximate top of bedrock, and PVC casing below. Descriptive logs of the OW are also available in the BC Ministry of Environment and Climate Change Strategy's groundwater wells and aquifers database (GWELLS; BC Ministry of Environment and Climate Change Strategy, 2020). Figure 2 shows the logs of OW 418, which was the deepest borehole logged. Note that the gamma-ray signal is somewhat attenuated in the steel-cased interval. In addition to those illustrated here, the logs for EERI-2 and -3 are shown in Monahan et al. (2020, Figures 3, 4).

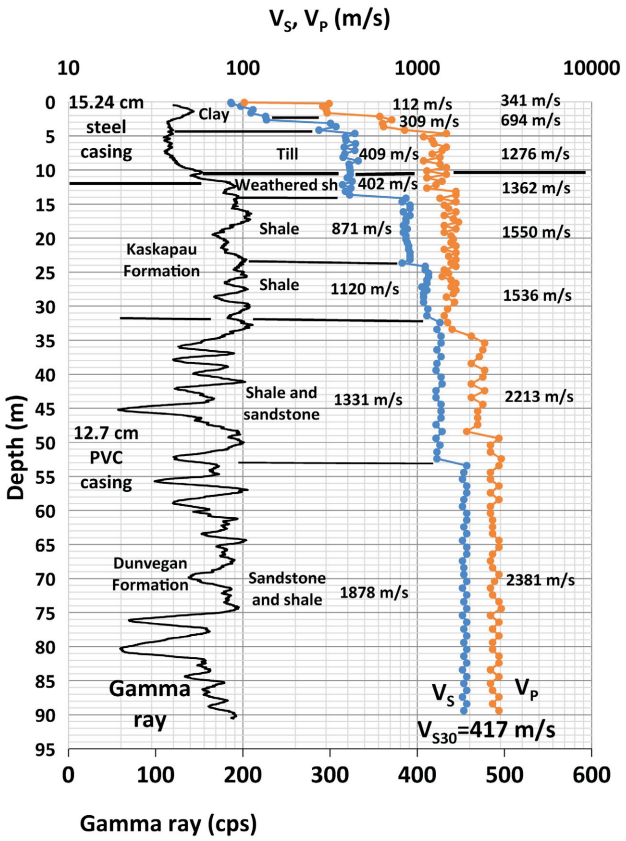


**Figure 2.** Borehole logs for Observation Well 418 (groundwater wells and aquifers database [GWELLS] well tag number 104709; BC Ministry of Environment and Climate Change Strategy, 2020), located on gently sloping upland hillside. Gamma-ray, shear-wave velocity ($V_S$) and P-wave velocity ($V_P$) data. Average $V_S$ and $V_P$ posted for each interval. Lithological log and descriptions modified from those of Kelly and Janicki (2103) and GWELLS to match gamma-ray and velocity logs. Note downward increase in $V_S$ below the weathered interval. Note also, attenuation of gamma-ray signal in steel-cased interval. Top of bedrock picked in this interval based on driller's log and the lower and less serrate gamma-ray signature of Quaternary till compared to Cretaceous shale. Upper part of Dunvegan Formation from 32 to 75 m correlates with the basal A-X member of the Kaskapau alloformation of Plint (2000). Gamma-ray scale at bottom. The average shear-wave velocity in upper 30 m ($V_{S30}$) is 417 m/s at the site (Site Class C). Abbreviations: cps, counts per second; PVC, polyvinyl chloride; sh, shale.

**Table 2.** Summary of vertical seismic profiling (VSP) data in pre-existing boreholes. All co-ordinates are in UTM Zone 10N, NAD 83. Locations of boreholes shown on Figure 1. Abbreviations: GWELLS, BC Ministry of Environment and Climate Change Strategy's groundwater wells and aquifers database; OW, observation well; $V_{S30}$, average shear-wave velocity in upper 30 m; WTN, well tag number.

| Borehole | Easting | Northing | Elevation (m asl) | Depth penetrated (m) | Depth to bedrock (m) | $V_{S30}$ (m/s) | Site Class | Setting | Reference |
|---|---|---|---|---|---|---|---|---|---|
| EERI-2 | 664116 | 6197620 | 747 | 45 | 26.7 | 271 | D | Gentle upland hillside | Cahill et al., 2019; Monahan et al., 2020 |
| EERI-3 | 623071 | 6239713 | 737 | 55 | 26 | 276 | D | Valley bottom | Cahill et al., 2019; Monahan et al., 2020 |
| OW 418 | 659177 | 6198989 | 699 | 91 | 10 | 417 | C | Gentle upland hillside | Kelly and Janicki, 2013 (GWELLS WTN 104709) |
| OW 420 | 664197 | 6187988 | 776 | 44 | 22.5 | 370 | C | Gentle upland hillside | Kelly and Janicki, 2013 (GWELLS WTN 104711) |
| EERI-7 | 668605 | 6199167 | 790 | 33 | 5.5 | 360 | C-D | Gentle upland hilltop | Ladd et al., 2019, 2020 |
| EERI-8 | 640811 | 6205544 | 824 | 32 | 2.5 | 415 | C | Steep upland hilltop | Ladd et al., 2019, 2020 |
| EERI-12 | 631468 | 6245003 | 691 | 32 | 19 | 500 | C | Steep upland hillside | Ladd et al., 2019, 2020 |

**Table 3.** Summary of multichannel analysis of surface wave (MASW) data. All co-ordinates are in UTM Zone 10N, NAD 83. Depth to bedrock is interpreted from gamma-ray log in adjacent petroleum well or borehole, except for those where the depth to bedrock was interpreted from the MASW profile (indicated with an asterisk).

| Test site | Seismic station/ wellsite/location | Elevation (m asl) | Easting | Northing | Depth penetrated (m) | Depth to bedrock (m) | $V_{S30}$ (m/s) | Site Class | Setting | Reference |
|---|---|---|---|---|---|---|---|---|---|---|
| SL19-1 | MONT1, South of Parkland Rd | 719 | 650841 | 6198716 | 38 | | 253 ±4 | D | Minor valley bottom - glaciolacustrine | Monahan et al., 2020 |
| SL19-2 | EERI 2 | 747 | 664110 | 6197627 | 34 | 26.7 | 228 ±7 | D | Gently sloping upland hillside | Cahill et al., 2019; Monahan et al., 2020 |
| SL19-3 | Proprietary seismic station, 11-11-80-16W6[1] | 722 | 663081 | 6200612 | 36 | | 345 ±14 | D | Steep upland hillside | |
| SL19-4 | MG05, 16-32-79-15W6 | 794 | 668701 | 6197690 | 30 | | 233 ±13 | D | Gentle upland hilltop | Monahan et al., 2020 |
| SL19-5 | MONT8 | 685 | 638350 | 6215777 | 36 | >36* | 246 ±16 | D | Gently sloping upland hillside | |
| SL19-6 | MG03, 14-4-80-16W6 | 699 | 659839 | 6199174 | 30 | 50.5 | 268 ±15 | D | Edge of minor valley bottom - glaciolacustrine | |
| SL19-7 | MG04, 6-6-81-15W6 | 681 | 666039 | 6208315 | 32 | 77.7 | 221 ±5 | D | Glaciolacustrine bench above Kiskatinaw River | |
| SL19-8 | MG02, 13-23-079-14W6 | 641 | 682467 | 6195094 | 32 | 67.2 | 238 ±15 | D | Glaciolacustrine bench | |
| SL19-9 | MG01, 16-30-81-17W6 | 721 | 647093 | 6214696 | 30 | 102.8 | 192 ±17 | D-E | Valley bottom, glaciolacustrine organic soils at surface | Hansen, 1950; Farstad et al., 1965; Lord and Greene, 1986 |
| SL19-10 | GSBC BH 2017-12 | 652 | 627001 | 6234050 | 32 | >53.6 | 303 ±8 | D | Glaciolacustrine bench above Peace River | Levson and Best, 2017 |
| SL19-11 | Wilder Gas Plant, 10-14-82-20W6, near MONT6 | 622 | 623627 | 6220351 | 30 | | 309 ±32 | D | Glaciolacustrine bench above Pine River | |
| SL19-12 | Terrace above Pine River | 514 | 620944 | 6216406 | 30 | | 292 ±5 | D | Glaciofluvial terrace above Pine River | |
| SL19-13 | West end Parkland Rd | 762 | 649412 | 6199166 | 30 | | 384 ±34 | C-D | Upland hilltop | |
| SL19-14 | MG10, Patterson Rd, Briar Ridge | 793 | 684376 | 6179103 | 30 | 18* | 287 ±18 | D | Gentle slope near upland hilltop | |
| SL19-15 | Northern Lights College, Dawson Creek Campus | 661 | 674114 | 6181275 | 30 | 13* | 386 ±20 | C | Minor valley bottom - glaciolacustrine | |
| SL19-16 | 226 Rd | 837 | 649114 | 6210336 | 30 | | 371 ±23 | C-D | Gentle upland slope near hilltop | |
| SL19-17 | Station 15, 11-28-80-18 | 797 | 639975 | 6204452 | 30 | 5* | 499 ±31 | C | Steep slope | Babaie Mahani and Kao, 2018 |
| SL19-18 | Lebell Road | 699 | 650083 | 6206051 | 30 | | 273 ±6 | D | Glaciolacustrine bench | |
| SL19-19 | West Doe Gas Plant, 2-11-80-16W6 | 703 | 663492 | 6199398 | 30 | 15* | 338 ±13 | D | Edge of minor valley bottom - glaciolacustrine | |
| SL19-20 | Station 9, 11-24-81-18W6 | 772 | 644574 | 6212594 | 30 | 48.2 | 259 ±18 | D | Gentle upland slope | Babaie Mahani and Kao, 2018 |
| SL19-21 | Airport Road, Fort St. John | 683 | 637354 | 6235899 | 30 | | 349 ±9 | D | Gentle upland terrane | |

[1] L.S. 11, Sec. 11, Twp. 80, Rge. 16, W 6th Mer.

The MASW profiles were acquired at 21 sites, and the results are summarized in Table 3. Of these, 11 were acquired at seismograph stations, in order to assess site effects: six are in the McGill University Dawson–Septimus Induced Seismicity Study network (MG01 to MG05 and M10; McGill University, 2020), two are in the Geological Survey of Canada–BC Oil and Gas Commission Induced Seismicity Study network (MONT1, MONT8; Natural Resources Canada, 2020), two are industry stations included in the study by Babaie Mahani and Kao (2018; stations 9 and 15), and one is a proprietary industry station. Six MASW profiles were acquired at residences (two co-located with seismograph stations), to calibrate the residents' experiences with induced earthquakes (MASW SL19-1, -12, -13, -14, -16, -18). Six MASW profiles were located adjacent to sites where geotechnical or scientific borehole data had been obtained, in order to refine the $V_S$ model of the shallow geological materials (MASW SL19-2, -10, -11, -15, -17, -21). One MASW, SL19-2, was done adjacent to EERI-2 in order to compare the two techniques.

The total depths investigated on the MASW profiles are between 30 and 38 m. The $V_S$ data are determined at multiple geophones on each profile (typically 39), so that $V_{S30}$ was calculated at each geophone, and the $V_{S30}$ mean and standard deviation could be calculated for the entire profile (Table 3). Note that the mean $V_{S30}$ shown in Table 3 is the time-averaged velocity in the top 30 m of the soil column at all geophones. The depths to bedrock reported are either interpreted from adjacent petroleum industry gamma-ray logs or other borehole data, or interpreted from the MASW data. An example of a MASW profile and adjacent borehole data are shown in Figure 3a, b.

## $V_S$ Model of Shallow Geological Deposits

The $V_S$ data acquired for this project have been used to prepare a $V_S$ model of the shallow geological deposits in the project area, and builds on a $V_S$ model developed previously for the entire Montney play area (Monahan et al., 2019). The new model incorporates $V_S$ data acquired for the previous study, including six VSP logs in the Groundbirch area, twelve MASW profiles (Figure 1), and three dipole sonic logs in Geoscience BC boreholes drilled in 2017. Four of the MASW profiles and all the dipole sonic logs are from outside of the current project area and not shown on Figure 1. All data from the previous study were reinterpreted for the new model. The data have been supplemented by $V_S$ data acquired by others, comprising nine seismic cone penetration tests (SCPT) at four sites, and four MASW tests at one site. Most of the latter data are proprietary. Of the five sites, only one is outside of the area shown in Figure 1.

To develop the model, the $V_S$ data points were correlated with specific stratigraphic units. In computing the average $V_S$ ($V_{SAV}$) for each unit, data were time-averaged to be consistent with the calculation of $V_{S30}$. For the borehole $V_S$ data, published core descriptions and wireline log data are sufficient to confidently assign $V_S$ data points to specific stratigraphic units (Figures 2, 4, 5). Core descriptions for these boreholes are by Hickin et al. (2016a; Groundbirch), Levson and Best (2017; Geoscience BC 2017 boreholes), and Goetz (Cahill et al., 2019; Ladd et al., 2019; EERI boreholes).

However, for the MASW profiles, only data from those adjacent to geotechnical or scientific boreholes were used—that is, all of the MASW profiles from Monahan et al. (2019) and six of the MASW profiles acquired for this study. In these, only intervals from the closest geophone to the borehole that could be equated with specific stratigraphic intervals in the boreholes were used in the $V_S$ model (e.g., Figure 3). Data from deeper than the bottom of the adjacent borehole were excluded, except in cases where bedrock had been confirmed in the borehole.

The $V_S$ model is summarized in Table 4. The ranges shown on the table are the lowest and highest interval values rather than from individual data points. Ranges of standard penetration test (SPT) blowcount (N) values for each stratigraphic unit were derived from geotechnical borehole data collected as part of the project (Monahan et al., 2020). The SPT blowcount is the number of hammer blows required to drive a sample tube 305 mm (1 ft.), and is a measure of the strength and consolidation of the deposits. The test is usually terminated after 50 blows, which is referred to as 'refusal'. The new $V_S$ model is generally similar to that previously described by Monahan et al. (2019), but differs from the earlier model in two important aspects—the greater range of $V_S$ for tills and weathered bedrock (shale and sandstone; Monahan et al., 2020).

### Holocene and Retreat-Phase Deposits of the Last Glaciation

Holocene alluvium was tested at one MASW site on the Sikanni Chief River, north of the project area (Monahan et al., 2019; SL2-2), where the $V_{SAV}$ is 196 ±14 m/s in 11 m of interbedded gravel, sand and silt. Based on a comparison with Holocene fluvial deposits elsewhere, this is likely to be representative of these deposits in the Fort St. John–Dawson Creek area.

Retreat-phase deposits of the last glaciation show a pattern of increasing $V_S$ with grain size. The $V_{SAV}$ increases from 214 ±55 m/s in glaciolacustrine silt, clay and very fine sand (25 sites), to 299 ±45 m/s in glaciolacustrine and glaciodeltaic sand with minor gravel (six sites), and to 364 ±91 m/s in glaciofluvial gravel and sand (one site). The last mentioned site is located on a glaciofluvial terrace and the gravel and sand is overlain by 7 m of thick silt. The $V_{SAV}$

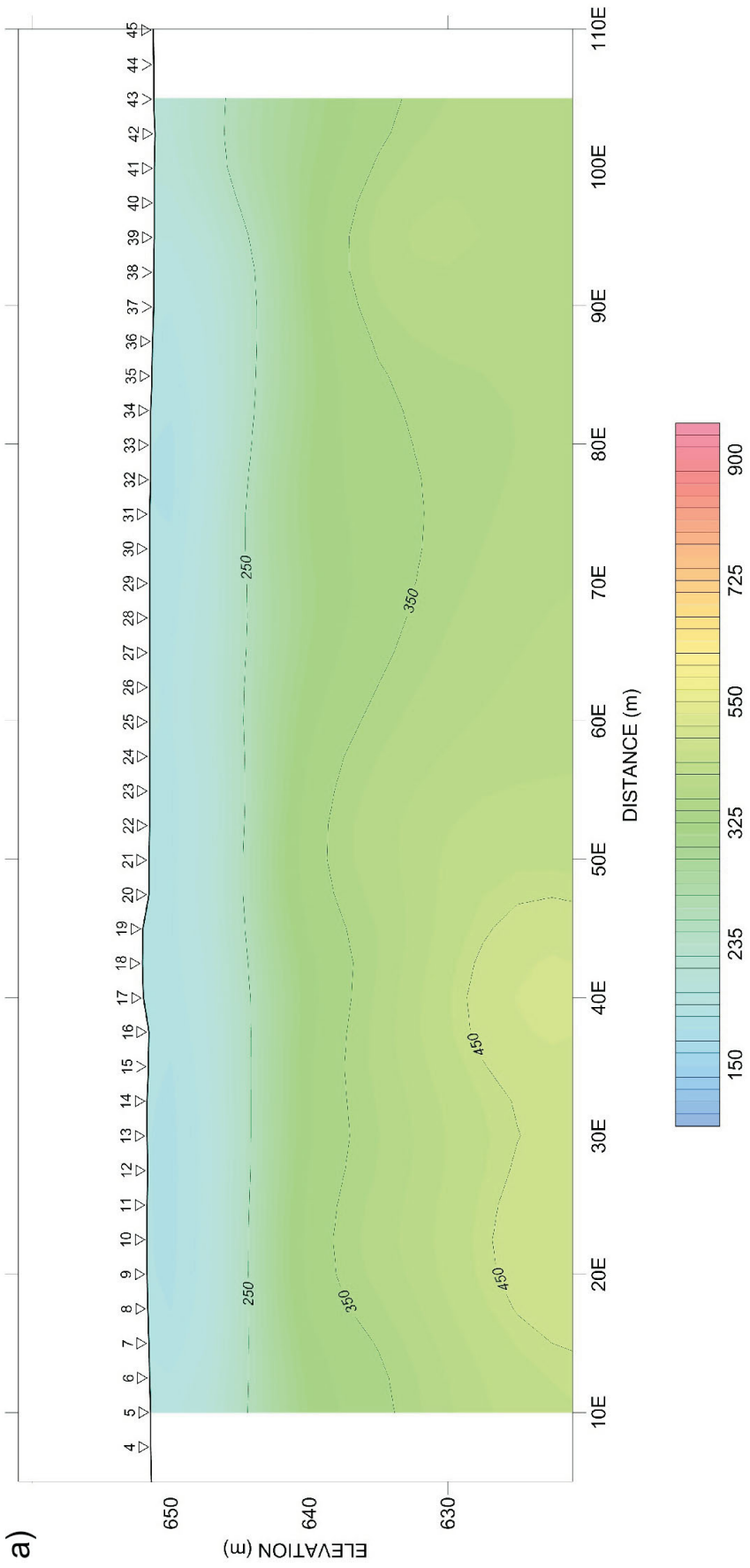


**Figure 3.** Multichannel analysis of surface waves (MASW) at SL19-10 at Geoscience BC borehole 2017-12 (Levson and Best, 2017), located on a glaciolacustrine bench above the Peace River. **a)** MASW profile. Numbers along the top of the profile are geophone locations. Abbreviation: E, east.

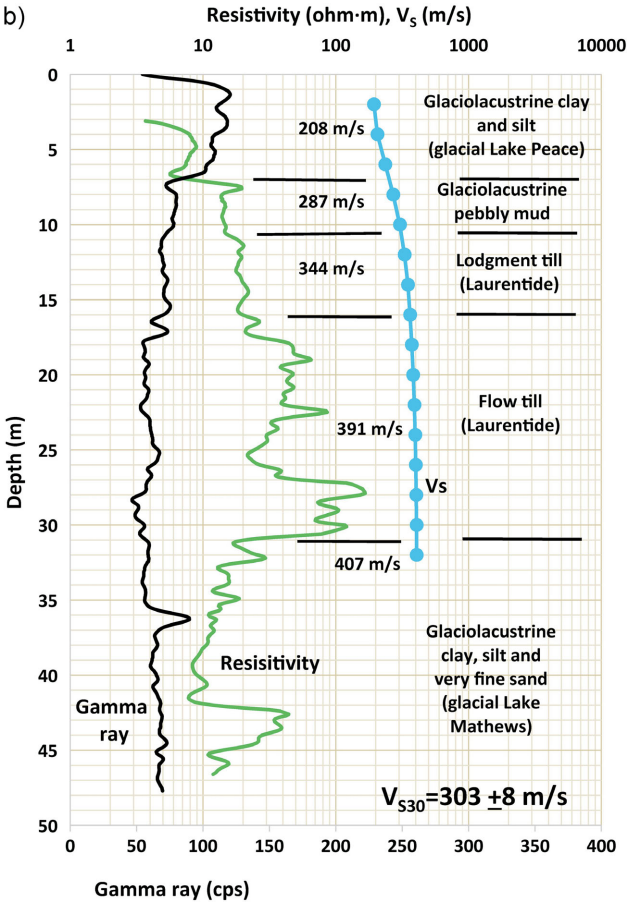


**Figure 3** (continued)**.** Multichannel analysis of surface waves (MASW) at SL19-10 at Geoscience BC borehole 2017-12 (Levson and Best, 2017), located on a glaciolacustrine bench above the Peace River. **b)** Borehole gamma-ray and resistivity logs and shear-wave velocity ($V_S$) trace at geophone 24 (627001E, 6234050N, UTM Zone 10N, NAD 83), the closest to the borehole. Average $V_S$ is posted for each interval. Gamma-ray and resistivity logs by Weatherford International plc, core description from Levson and Best (2017). The average shear-wave velocity in upper 30 m ($V_{S30}$) is 303 ±8 m/s at the site (Site Class D).

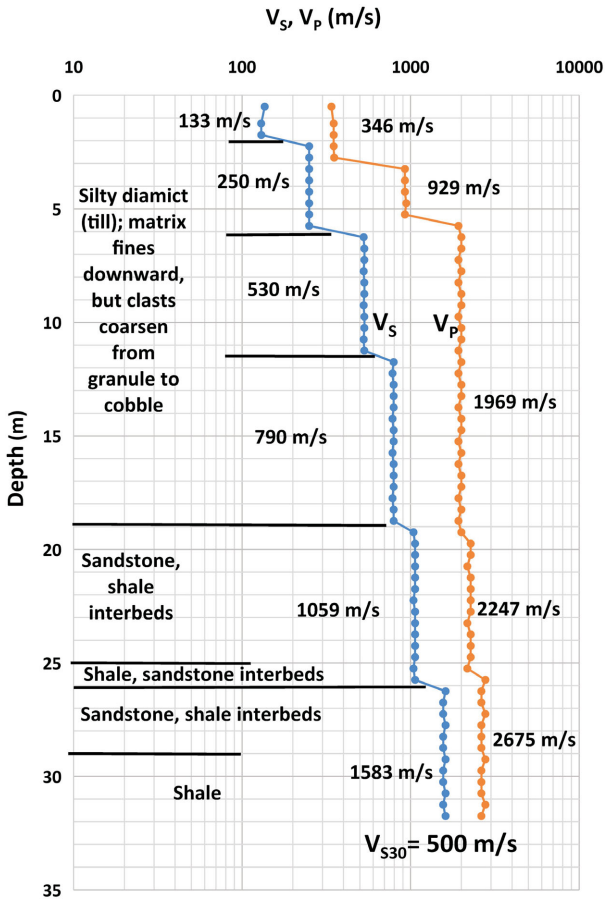


**Figure 4.** Borehole log for EERI-12. Shear-wave velocity ($V_S$) and P-wave velocity ($V_P$) data. Average $V_S$ and $V_P$ are posted for each interval. Core description by Goetz (in Ladd et al., 2019). Note that the $V_S$ increases downward through the diamict (i.e., till) as clast size increases. The $V_S$ increase at 12.5 m is interpreted to represent the downward change from meltout to lodgment till. An alternate interpretation is that each $V_S$ interval represents a till of a different age. The average shear-wave velocity in upper 30 m ($V_{S30}$) is 500 m/s at the site (Site Class C).

of these deposits together is 326 ±94 m/s. Pebbly silt intervals interbedded with glaciolacustrine sediments are 3 to 7 m thick and have a $V_{SAV}$ of 301 ±29 m/s (three sites; e.g., Figure 3b).

Retreat-phase glaciolacustrine silt, clay and very fine sand are widespread and described in many geotechnical boreholes. The SPT N values are generally between 2 and 20 for these deposits.

## Tills

Till occurs in 42 intervals at 30 sites and has a $V_{SAV}$ of 343 ±176 m/s. However, the till intervals can be subdivided into those interpreted to be Late Wisconsinan, which occur at surface or directly below the Late Wisconsinan retreat-phase deposits, and those that occur deeper in the section and are interpreted to be older.

Accordingly, till intervals at 28 sites are interpreted as Late Wisconsinan and have a $V_{SAV}$ of 321 ±134 m/s, with a wide range from 135 to 790 m/s. In most borehole logs, the differentiation between meltout, flow and lodgment till was not made by the person logging the core. However, these interpretations were made by Hickin et al. (2016a) and Levson and Best (2017) in their core descriptions (e.g., Figure 3); and in two of the EERI borehole logs the distinction between meltout and lodgment till can be inferred from an abrupt downward increase in $V_S$ in an otherwise continuous till sequence (Figure 4). Following these interpretations, Late Wisconsinan meltout till occurs at two sites with $V_{SAV}$ of 224 ±52 m/s, flow till occurs at two sites with $V_{SAV}$ of 377 ±42 m/s, and lodgment till at eight sites with $V_{SAV}$ of 422 ±151 m/s. Undifferentiated tills at 20 sites have a $V_{SAV}$ of 295 ±110 m/s. Significantly, the range of $V_{SAV}$ in till in the thick till blanket encountered in many upland sites in the eastern part of the project area overlaps with that of gla-

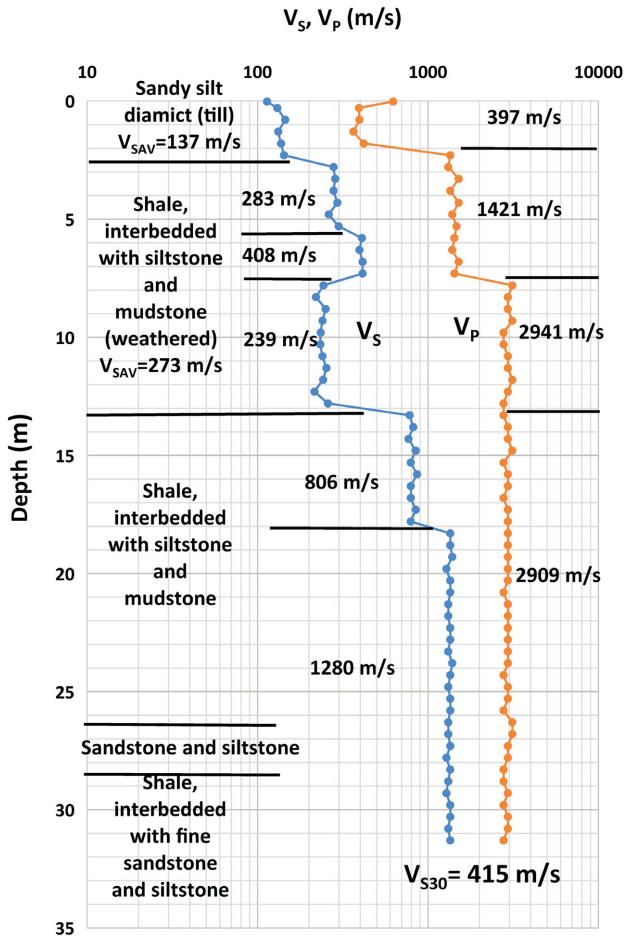


**Figure 5.** Borehole log for EERI-8, located on steep upland hilltop. Shear-wave velocity ($V_S$) and P-wave velocity ($V_P$) data. Average $V_S$ and $V_P$ are posted for each interval. Core description by Goetz (Ladd et al., 2019). Note weathered bedrock interval is 10.5 m thick with an average shear-wave velocity ($V_{SAV}$) of 273 m/s. The average shear-wave velocity in upper 30 m ($V_{S30}$) is 415 m/s at the site (Site Class C).

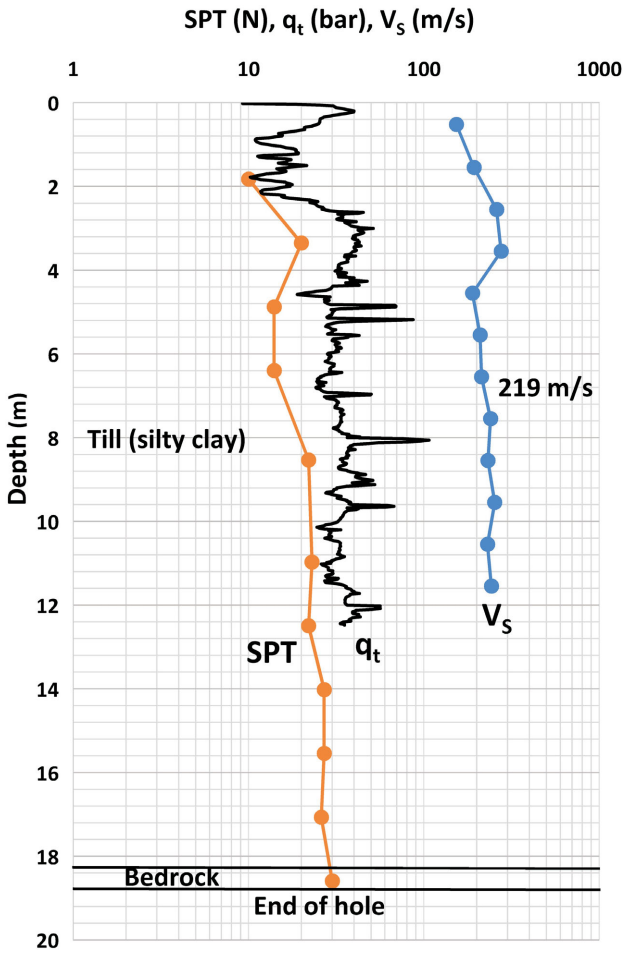


**Figure 6.** Proprietary data from a geotechnical investigation at a gently sloping upland site, provided courtesy of an oil and gas operator. Data shown are shear-wave velocity ($V_S$) and tip resistance (qt) from a seismic cone penetration test (SCPT). Standard penetration test (SPT) blowcount (N) and lithological data are from an adjacent borehole. Average $V_S$ in the SCPT is 219 m/s. Based on a correlation of N with $V_S$, the average $V_S$ of the section down the bottom of the borehole is estimated to be 224 m/s, and estimated average shear-wave velocity in upper 30 m ($V_{S30}$) is 312 m/s, assuming bedrock $V_S$ of 900 m/s from the base of the hole down to 30 m (Site Class D). This estimate is an upper bound one, as the one bedrock N value (30) indicates that the bedrock surface is weathered, and the estimated $V_{S30}$ will be less if a thick weathered interval is present.

ciolacustrine silt (e.g., Figure 6). In geotechnical boreholes, the range of SPT N values in Late Wisconsinan tills is typically between 10 and >50 (i.e., refusal).

Tills interpreted to be older than the last glacial maximum occur at four sites, and have a $V_{SAV}$ of 660 ±132 m/s. Lodgment till occurs at three sites with a $V_{SAV}$ of 709 ±100 m/s, and flow till occurs at two sites with a $V_{SAV}$ of 572 ±111 m/s (Hickin et al., 2016a; Levson and Best, 2017; Monahan et al., 2019).

The range of $V_{SAV}$ in tills is likely related to varying degrees of glacial compaction and clast and clay content, with the latter increasing and decreasing $V_S$, respectively. Although till provenance controls lithology, and Laurentide tills are clay rich (Mathews, 1978), there are insufficient data to assess the control of provenance on till $V_S$.

## Advance-Phase Deposits of the Last Glaciation and Earlier Deposits

Deposits older than the Late Wisconsinan glacial maximum are represented at 10 sites. These have higher $V_{SAV}$ than retreat-phase and Holocene deposits due to glacial compaction, and display less grain-size control of $V_S$. Glaciolacustrine clay, silt and very fine sand occur at six sites, with a $V_{SAV}$ of 426 ±26 m/s; glaciolacustrine and glaciodeltaic silty sand and sand occur at five sites, with a $V_{SAV}$ of 527 ±188 m/s; and glaciofluvial and fluvial sand and gravel occur at seven sites with a $V_{SAV}$ of 519 ±117 m/s.

**Table 4.** Shear-wave velocity ($V_S$) model of near-surface geological deposits in the Fort St. John–Dawson Creek area. Numbers in brackets in environment and lithology columns are the number of sites represented. Bracketed standard penetration test (SPT) blow-count (N) values are inferred, not observed. Ranges in $V_S$ are highest and lowest interval averages, rather than individual data points.

| Period | Unit | Environments | Lithology | SPT N | $V_S$ average (range, m/s) |
|---|---|---|---|---|---|
| Holocene | Alluvium | | Silt, sand and gravel (1) | 14–25 (>50?) | 196 ±14 (180–250?) |
| Pleistocene | Late Wisconsinan glaciation retreat phase | Glaciofluvial terrace | Gravel and sand (1) (with overlying silt $V_{SAV}$ 326 ±94) | | 364 ±91 (260–400) |
| | | Glaciolacustrine | Silt, clay and very fine sand (25) | 2 to 20 | 214 ±55 (135–330) |
| | | | Pebbly silt (3) | | 301 ±29 (285–340) |
| | | Glaciolacustrine, glaciodeltaic | Sand and gravel (6) | (20 to 50) | 299 ±45 (250–370) |
| | | Tills (28 sites) $V_{SAV}$ 321 ±134 (135–790) | Flow till (2) | | 377 ±42 333–465 |
| | | | Meltout till (2) | | 224 ±52 (135–260) |
| | Late Wisconsinan glaciation maximum | | Undifferentiated till (20) | 10 to >50 | 295 ±110 (135–600) |
| | | | Lodgment till (8) | | 422 ±151 (260–790) |
| | Late Wisconsinan advance phase and earlier glacial and nonglacial deposits | Glaciolacustrine | Clay, silt and very fine sand (6) | 15 to >50 | 426 ±26 (360–460) |
| | | Glaciolacustrine, glaciodeltaic | Silty sand and sand (5) | (>50) | 527 ±188 (400–860) |
| | | Glaciofluvial and fluvial | Gravel and sand (7) | (>50) | 519 ±117 (420–840) |
| | | Tills | Till, flow and lodgment (4) | (>50) | 660 ±132 (490–830) |
| Cretaceous | Cardium, Kaskapau, Dunvegan and Shaftesbury fm. | Weathered shale and sandstone (16) | | 30 to >50 | 522 ±232 (240–1200) |
| | | Shale (7) | | >50 | 962 ±198 (725–1280) |
| | | Interbedded sandstone and shale (9) | | >50 | 1179 ±411 (725–1878) |

## Bedrock

Bedrock $V_S$ was recorded at 18 sites. Weathered intervals at the top of bedrock occur at 16 sites and were either directly reported on borehole logs (e.g., Figure 5) or interpreted on MASW profiles by steep downward $V_S$ increases before levelling off at a high $V_S$, with the latter being interpreted as unweathered bedrock (e.g., Figure 7). Weathered intervals are up to 36 m thick, with an average of 15 m and a $V_{SAV}$ of 522 ±232 m/s.

Relatively unweathered bedrock is represented at 11 sites. Shale intervals have generally lower $V_{SAV}$ than intervals of interbedded sandstone and shale. The $V_{SAV}$ for these intervals are 962 ±198 m/s and 1179 ±411 m/s, respectively. However, $V_S$ continues to increase downward from the weathered zone, as shown in OW 418, where $V_{SAV}$ increases downward from 871 m/s at 14 to 24 m depth in Kaskapau Formation shale to 1878 m/s between 53 and 90 m in the Dunvegan Formation sandstone and shale (Figure 2). This downward increase is likely due to the gradually decreasing effects of weathering below the upper highly weathered interval, the closure of fractures due to greater overburden stress and the effect of increased overburden stress itself.

## $V_{S30}$ by Geomorphological Setting

Figure 8 shows the distribution of $V_{S30}$ by geomorphological setting at sites in the Fort St. John–Dawson Creek area. Those sites on modern alluvium, glaciofluvial terraces and glaciolacustrine benches and minor valley floors are generally in Site Class D, as would be expected as these deposits are generally relatively thick and/or overlie

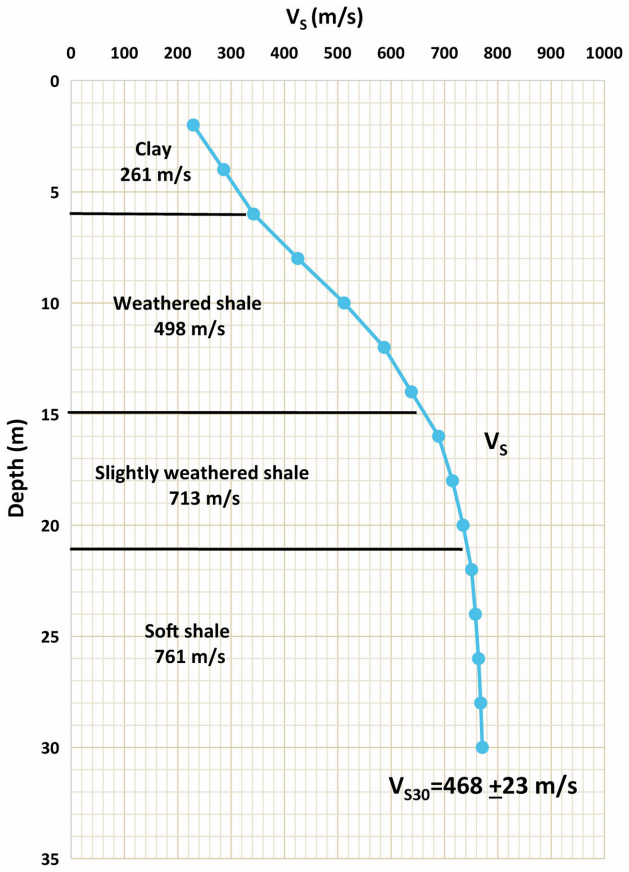


**Figure 7.** Shear-wave velocity ($V_S$) trace from multichannel analysis of surface waves (MASW) at test site SL-4, from previous study (Monahan et al., 2019), and lithological data from adjacent proprietary borehole. Site located at hilltop site of gentle topography in Dawson Creek. The $V_S$ trace is at geophone 28, the closest to the borehole (673711E, 6184226N, UTM Zone 10N, NAD 83). Average $V_S$ is posted for each interval. Borehole log reports weathered shale down to 15 m, but the $V_S$ trace suggests that the effects of weathering extend down to ~21 m. Relatively unweathered bedrock is interpreted below 21 m where the $V_S$ values level off at high values. The average shear-wave velocity in upper 30 m ($V_{S30}$) is 468 ±23 at the site (Site Class C).

older Quaternary deposits. At the two glaciolacustrine sites in Site Class C, which are located in minor valleys, bedrock is interpreted to be shallow (<20 m) on the MASW profiles. Site Class in the upland sites ranges from B to D and overlaps with the glaciolacustrine sites where thick tills with $V_S$ comparable to glaciolacustrine deposits occur. This is particularly so in the uplands of subdued topography in the eastern part of the project area. However, $V_{S30}$ increases as depth to bedrock decreases, so in the steeper upland areas of the western part of the project area, where thin tills overlie bedrock, sites are likely to be in Site Class C.

The relationship between $V_{S30}$ and depth to bedrock is shown in Figure 9. Generally, sites where depth to bedrock exceeds 15 m are in Site Class D. Upland sites which deviate from this trend are associated with very high till velocities (e.g., EERI-12, Figure 4), or thick weathered bedrock intervals (e.g., EERI-7, -8; Figure 5).

The steeper upland areas, where bedrock is shallow and Site Class C predominates, are primarily underlain by sandstone units of the Dunvegan Formation and sandstone members of the Kaskapau Formation. These units are more resistant to erosion than shale of Kaskapau Formation, which underlies most of the upland areas of subdued topography in the eastern part of the project area, where thicker till overlies bedrock and Site Class D is widespread.

However, significant amplification of seismic ground motions may also occur due to resonance where the depth to bedrock is less than 15 m. Amplification of induced seismicity at the Groningen gas field in the Netherlands is greatest where Holocene deposits are thin (<~20 m), less so where they are thick, and the least where the Holocene is absent (van Ginkel et al., 2019).

## Conclusions

The project data confirm that, in the Fort St. John–Dawson Creek area, the shear-wave velocity of the clay-rich Late Wisconsinan till is commonly comparable to that of the Late Wisconsinan retreat-phase glaciolacustrine clay, silt and fine sand. Consequently, where thick till occurs in the upland areas of subdued topography, such as in the eastern part of the area, the average shear-wave velocity in the upper 30 m ($V_{S30}$) is similar to that of glaciolacustrine sites, and is assigned to Site Class D. In upland areas of steeper topography, where thinner tills overlie bedrock, Site Class C predominates. As a result, depth to bedrock is a better predictor of $V_{S30}$ than whether till or glaciolacustrine deposits occur at surface, and a depth of 15 m approximates the boundary between Site classes C and D. This depth may vary depending on the presence of denser till or a thick weathered bedrock interval with low velocity, which would increase or decrease, respectively, the bedrock depth of the Site Class C–D boundary.

However, amplification of seismic ground motions may also occur due to resonance where the depth to bedrock is less than 15 m. To assess this, future work in this project will include analysis of recorded ground motions at sites where the depth to bedrock is known.

## Acknowledgments

The authors gratefully thank the following organizations and individuals for:

- providing project funding: Geoscience BC;
- assistance in acquiring proprietary geotechnical borehole data: Metro Testing + Engineering Ltd. | Northern Geo Testing and Engineering; Urban Systems; City of Fort St. John; City of Dawson Creek; District of Taylor; Peace River Regional District; School Board 59: Peace River South; School Board 60: Peace River North; BC Hydro; BC Oil and Gas Commission; BC Ministry of Transportation and Infrastructure; Shell Canada Lim-

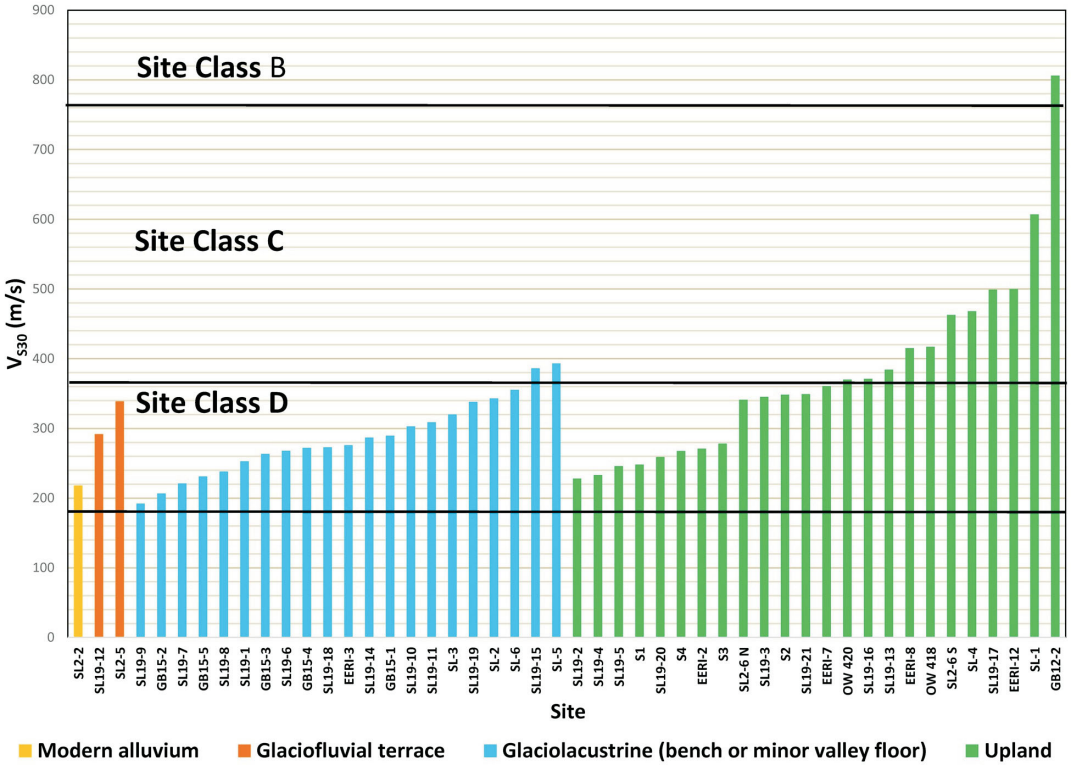


**Figure 8.** The average shear-wave velocity in the upper 30 m ($V_{S30}$) by geological setting for sites in the Fort St. John–Dawson Creek area. Only site SL2-2 is located outside of the project area; it represents a modern alluvium site. Site details are shown in Tables 2 and 3; sites SL-1 to SL-6, SL2-2, SL2-5, SL2-6 N, SL2-6 S, GB12-2 and GB15-1 to GB-15-5 are from a previous study by Monahan et al. (2019); data from tests S1 to S4 are proprietary. Note range of $V_{S30}$ in upland setting extends into Site Class D, overlapping with $V_{S30}$ of the other settings represented.

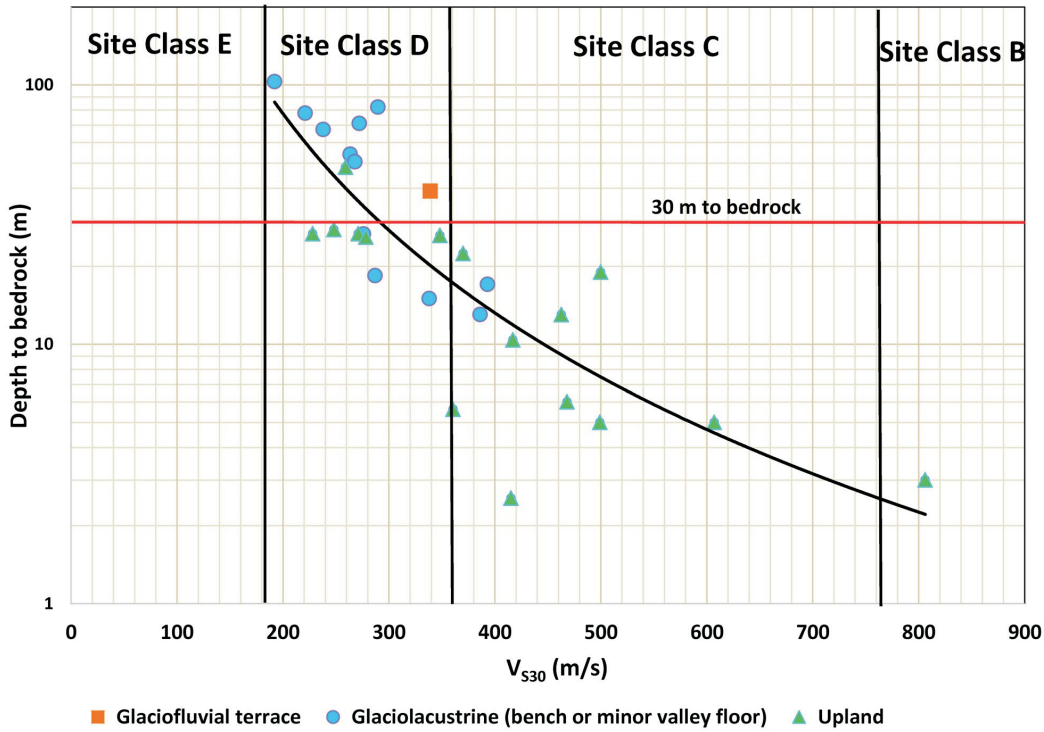


**Figure 9.** Plot of average shear-wave velocity in the upper 30 m ($V_{S30}$) versus depth to bedrock for sites in the Fort St. John–Dawson Creek area. Only sites where bedrock is confirmed in the boreholes are shown. Power trendline is for all points, $R^2$=0.69. Note that for sites where bedrock is deeper than 30 m, shear-wave velocity values below 30 m do not contribute to $V_{S30}$ calculation.

ited; ARC Resources Ltd.; Crew Energy Inc.; Ovintiv Inc.; Canadian Natural Resources Ltd.; Leucrotta Exploration Inc.; Tervita Corporation; The University of British Columbia's (UBC) Energy and Environment Research Initiative (EERI) Program; AltaGas Canada Ltd.; Golder Associates Ltd.; SBA Communications Corporation; Krahn Engineering Ltd.; Varcon Inc.; particular thanks to B. Rodowski, B. Ladd, J. Cegnar, S. Gaib and W. Lemky;

- access to field sites: UBC EERI Program, BC Ministry of Forests, Lands, Natural Resource Operations and Rural Development; McGill University Dawson–Septimus Induced Seismicity Project; BC Oil and Gas Commission; Tourmaline Oil Corp.; Northern Lights College; ARC Resources Ltd.; Crew Energy Inc.; Canadian Natural Resources Limited; Ovintiv Inc.; Shell Canada Limited; particular thanks to L. Hurrell, M. Goetz, G. Langston, A. Babaie Mahani, K. Evers, R. Nakamoto, D. McHarg and several residents, who granted access to their lands;
- helpful discussions: A. Babaie Mahani, S. Venables, J. Johnson, A.S. Hickin, J. Clague, W. Westwood, P. McLellan, J. van Besouw, K. Hadavi, T. Ferbey, B. Ard and C. Salas;
- assembling the manuscript: L. Sears;
- reviewing the manuscript: K. Dorey, A. Babaie Mahani and C. Salas;
- generating the proprietary shear-wave velocity data: ConeTec Inc., Golder Associates Ltd. and GeoNorth Engineering Ltd.;
- generating the proprietary geotechnical borehole logs used in the shear-wave velocity model: Metro Testing and Engineering Ltd. | Northern Geo Testing and Engineering, Aurora Engineering & Construction Services Ltd., Smith + Andersen (Kelowna), Wood PLC and predecessors, BC Hydro, SNC-Lavalin Group Inc., Harder Associates Engineering Consulting Inc., Golder Associates Ltd. and GeoNorth Engineering Ltd.

## References

Arsenault, J.-L., Hunter, J.A. and Crow, H.L. (2012): Shear wave velocity logs from vertical seismic profiles; *in* Shear Wave Velocity Measurement Guidelines for Canadian Seismic Site Characterization in Soil and Rock, J.A. Hunter and H.L. Crow (ed.), Geological Survey of Canada, Open File 7078, p. 123–138, URL <https://doi.org/10.4095/291753>.

Atkinson, G.M., Eaton, D.W., Ghofrani, H., Walker, D., Cheadle, B., Schultz, R., Shcherbakov, R., Tiampo, K., Gu, J., Harrington, R.M., Liu, Y., van der Baan, M. and Kao, H. (2016): Hydraulic fracturing and seismicity in the Western Canada Sedimentary Basin; Seismological Research Letters, v. 87, no. 3, p. 1–17, URL <https://www.desmogblog.com/sites/beta.desmogblog.com/files/Hydraulic%20Fracturing%20and%20Seismicity%20in%20the%20Western%20Canada%20Sedimentary%20Basin.pdf> [November 2020].

Babaie Mahani, A. and Kao, H. (2018): Ground motion from M 1.5 to 3.8 induced earthquakes at hypocentral distance <45 km in the Montney play of northeast British Columbia, Canada; Seismological Research Letters, v. 89, no. 1, p. 22–34, URL <https://doi.org/10.1785/0220170119>.

Babaie Mahani, A., Kao, H., Atkinson, G.M., Assatourians, K., Addo, K. and Liu, Y. (2019): Ground-motion characteristics of the 30 November 2018 injection-induced earthquake sequence in northeast British Columbia, Canada; Seismological Research Letters, v. 90, no. 4, p. 1457–1467, URL <https://doi.org/10.1785/0220190040>.

Babaie Mahani, A., Kao, H., Johnson, J. and Salas, C. (2017a): Ground motion from the August 17, 2015, moment magnitude 4.6 earthquake induced by hydraulic fracturing in northeastern British Columbia; *in* Geoscience BC Summary of Activities 2016, Geoscience BC, Report 2017-01, p. 9–14, URL <http://www.geosciencebc.com/i/pdf/SummaryofActivities2016/SoA2016_BabaieMahani.pdf> [October 2017].

Babaie Mahani, A., Schultz, R., Kao, H., Walker, D., Johnson, J. and Salas, C. (2017b): Fluid injection and seismic activity in the northern Montney play, British Columbia, Canada, with special reference to the 17 August 2015 Mw 4.6 induced earthquake; Bulletin of the Seismological Society of America, v. 107, p. 542–552, URL <https://doi.org/10.1785/0120160175>.

BC Ministry of Environment and Climate Change Strategy (2020): Groundwater wells and aquifers (GWELLS) database; BC Ministry of Environment and Climate Change Strategy, URL <https://apps.nrs.gov.bc.ca/gwells/> [September 2020].

Building Seismic Safety Council (2003): NEHRP recommended provisions for seismic regulations for new buildings and other structures (FEMA 450), part 1: provisions (2003 edition); prepared for the Federal Emergency Management Agency, 338 p., URL <http://www.nehrp.gov/pdf/fema450-provisions.pdf> [October 2017].

Cahill, A.G., Beckie, R.D., Goetz, M., Allen, A., Ladd, B., Welch, L., Kirste, D., Mayer, B. and van Geloven, C. (2019): Characterizing dissolved methane in groundwater in the Peace Region, northeastern British Columbia, using a regional, dedicated, groundwater monitoring well network; *in* Geoscience BC Summary of Activities 2018: Energy and Water, Geoscience BC, Report 2019-02, p. 105–122, URL <http://cdn.geosciencebc.com/pdf/SummaryofActivities2018/EW/2017-002_SoA2018_EW_Cahill_DissolvedMethane.pdf> [November 2020].

Farstad, L., Lord, T.M., Green, A.J. and Hortie, H.J. (1965): Soil survey of the Peace River area in British Columbia; University of British Columbia, British Columbia Department of Agriculture and Canada Department of Agriculture, Research Branch, British Columbia Soil Survey Report No. 8, 114 p., URL <http://www.env.gov.bc.ca/esd/distdata/ecosystems/Soils_Reports/bc8_report.pdf> [November 2020].

Finn, W.D.L. and Wightman, A. (2003): Ground motion amplification factors for the proposed 2005 edition of the National Building Code of Canada; Canadian Journal of Civil Engineering, v. 30, p. 272–278, URL <https://cdnsciencepub.com/doi/pdf/10.1139/l02-081> [November 2020].

Hansen, H.P. (1950): Postglacial forests along the Alaska Highway in British Columbia; Proceedings of the American Philosophical Society, v. 94, no. 5, p. 411–421.

Hartman, G.M.D. and Clague, J.J. (2008): Quaternary stratigraphy and glacial history of the Peace River valley, northeast Brit-

ish Columbia; Canadian Journal of Earth Sciences, v. 45, p. 549–564, URL <https://cdnsciencepub.com/doi/pdf/10.1139/E07-069> [November 2020].

Hartman, G.M.D., Clague, J.J., Barendregt, R.W. and Reyes, A.V. (2018): Late Wisconsinan Cordilleran and Laurentide glaciation of the Peace River Valley east of the Rocky Mountains, British Columbia; Canadian Journal of Earth Sciences, v. 55, no. 12, p. 1324–1338, URL <https://doi.org/10.1139/cjes-2018-0015>.

Hickin, A.S., Best, M.E. and Pugin, A. (2016a): Geometry and valley-fill stratigraphic framework for aquifers in the Groundbirch paleovalley assessed through shallow seismic and ground-based electromagnetic surveys; BC Ministry of Energy, Mines and Low Carbon Innovation, BC Geological Survey, Open File 2016-5, 46 p., URL <http://cmscontent.nrs.gov.bc.ca/geoscience/PublicationCatalogue/OpenFile/BCGS_OF2016-05.pdf> [November 2020].

Hickin, A.S., Lian, O.B. and Levson, V.M. (2016b): Coalescence of late Wisconsinan Cordilleran and Laurentide ice sheets east of the Rocky Mountain Foothills in the Dawson Creek region, northeast British Columbia, Canada; Quaternary Research, v. 85, p. 409–429, URL <https://doi.org/10.1016/j.yqres.2016.02.005>.

Hickin, A.S., Lian, O.B., Levson, V.M. and Cui, Y. (2015): Pattern and chronology of glacial Lake Peace shorelines and implications for isostasy and ice-sheet configuration in northeastern British Columbia, Canada; Boreas, v. 44, p. 288–304, URL <https://doi.org/10.1111/bor.12110>.

Holland, S.S. (1976): Landforms of British Columbia – a physiographic outline; BC Ministry of Energy, Mines and Low Carbon Innovation, Bulletin 48, 138 p., URL <https://www2.gov.bc.ca/gov/content/industry/mineral-exploration-mining/british-columbia-geological-survey/publications/bulletins> [November 2020].

Hollingshead, S. and Watts, B.D. (1994): Preliminary seismic microzonation assessment for British Columbia; prepared for Resources Inventory Committee, Earth Sciences Task Force, 109 p.

Irish, E.J.W. (1958): Charlie Lake, West of Sixth Meridian, British Columbia; Geological Survey of Canada, Preliminary Map 17-1958, scale 1:253 440, 1 sheet, URL <https://doi.org/10.4095/106866>.

Kao, H., Hyndman, R., Jiang, Y., Visser, R., Smith, B., Babaie Mahani, A., Leonard, L., Ghofrani, H. and He, J. (2018): Induced seismicity in western Canada linked to tectonic strain rate: implications for regional seismic hazard; Geophysical Research Letters, v. 45, 12 p., URL <https://doi.org/10.1029/2018GL079288>.

Kelly, J. and Janicki, E. (2013): Drilling and construction of Provincial Observation Wells in the Montney play area, Dawson Creek, British Columbia 2011; BC Ministry of Environment and Climate Change Strategy, BC Ministry of Energy, Mines and Low Carbon Innovation, 84 p., URL <http://a100.gov.bc.ca/pub/acat/public/viewReport.do?reportId=36194> [November 2020].

Kramer, S.L. (1996): Geotechnical Earthquake Engineering; Prentice-Hall, Inc., Upper Saddle River, New Jersey, 653 p.

Ladd, B., Cahill, A.G., Goetz, M., Allen, A., Welch, L., Mayer, B., van Geloven, C., Kirste, D. and Beckie, R.D. (2020): Installation of a purpose-built groundwater monitoring well network to characterize groundwater methane in the Peace Region, northeastern British Columbia (NTS 093P/09–16, 094A/01–08); *in* Geoscience BC Summary of Activities 2019: Energy and Water, Geoscience BC, Report 2020-02, p. 131–144, URL <http://www.geosciencebc.com/i/pdf/SummaryofActivities2019/EW/Project%202017-002_EW_SOA2019.pdf> [November 2020].

Ladd, B., Goetz, M., Allen, A., Kirste, D. and Beckie, R.D. (2019): Characterizing dissolved methane in groundwater in the Peace Region, Northeast BC, using a regional, dedicated groundwater monitoring well network, EERI Monitoring Well Installation Project (EERI MWIP), drilling campaign #3– review; The University of British Columbia, Energy and Environment Initiative, unpublished internal report, 20 p.

Levson, V. and Best, M. (2017): Northeast BC sonic drilling project, physical logs descriptions and interpretations; Geoscience BC, Geoscience BC Report 2017-16, 35 p., URL <http://cdn.geosciencebc.com/project_data/GBCR2017-16-CoreDescriptionsInterpretations.pdf> [November 2020].

Lord, T.M. and Green, A.J. (1986): Soils of the Fort St. John-Dawson Creek area, British Columbia; Canada Department of Agriculture, British Columbia Soil Survey Report No. 42, 81 p., URL <http://www.env.gov.bc.ca/esd/distdata/ecosystems/Soils_Reports/bc42_report.pdf> [November 2020].

Mathews, W.H. (1978): Quaternary stratigraphy and geomorphology of the Charlie Lake (94A) map-area, British Columbia; Geological Survey of Canada, Paper 76-20, 25 p., includes Map 1460A, scale 1:250 000, URL <https://geoscan.nrcan.gc.ca/starweb/geoscan/servlet.starweb?path=geoscan/downloade.web&search1=R=104544> [November 2020].

Mathews, W.H. (1980): Retreat of the last ice sheets in northeastern British Columbia and adjacent Alberta; Geological Survey of Canada, Bulletin 331, 22 p., URL <https://geoscan.nrcan.gc.ca/starweb/geoscan/servlet.starweb?path=geoscan/downloade.web&search1=R=102160> [November 2020].

McGill University (2020); McGill Dawson–Septimus Induced Seismicity Study; International Federation of Digital Seismograph Networks, URL <https://www.fdsn.org/networks/detail/XL_2017/> [November 2020].

McMechan, M.E. (1994): Geology and structure cross section, Dawson Creek, British Columbia; Geological Survey of Canada, Map 1858A, scale 1:250 000, URL <https://doi.org/10.4095/203491>.

Monahan, P.A., Hayes, B., Perra, M., Mykula, Y., Clarke, J., Galambos, B., Griffiths, D., Bayarsaikhan, O. and Oki, U. (2020): Amplification of seismic ground motion in the Fort St. John–Dawson Creek area, northeastern British Columbia; *in* Geoscience BC Summary of Activities 2019, Geoscience BC, Report 2020-02, p. 1–12, URL <http://www.geosciencebc.com/i/pdf/SummaryofActivities2019/EW/Project%202018-052_EW_SOA2019.pdf> [November 2020].

Monahan, P.A., Levson, V.M., Hayes, B.J., Dorey, K., Mykula, Y., Brenner, R., Clarke, J., Galambos, B., Candy, C., Krumbiegel, C. and Calderwood, E. (2019): Mapping the susceptibility to amplification of seismic ground motions in the Montney play area of northeastern British Columbia; Geoscience BC Report 2018-16, 65 p., URL <http://cdn.geosciencebc.com/project_data/GBCR2018-16/GBCR2018-16-NEBC_Amplification_Report.pdf> [November 2020].

National Research Council (2015): National Building Code of Canada; National Research Council, Ottawa, v. 1, 708 p.

Natural Resources Canada (2020): Geological Survey of Canada–BC Oil and Gas Commission Induced Seismicity Study; International Federation of Digital Seismograph Networks, URL <https://www.fdsn.org/networks/detail/1E_2018/> [November 2020].

Phillips, C. and Sol, S. (2012): Multichannel analysis of surface waves (MASW) technique for hazard studies; *in* Shear Wave Velocity Measurement Guidelines for Canadian Seismic Site Characterization in Soil and Rock, J.A. Hunter and H.L. Crow (ed.), Geological Survey of Canada, Open File 7078, p. 62–66, URL <https://doi.org/10.4095/291753>.

Plint, A.G. (2000): Sequence stratigraphy and paleogeography of a Cenomanian deltaic complex: the Dunvegan and lower Kaskapau formations in subsurface and out crop, Alberta and British Columbia, Canada; Bulletin of Canadian Petroleum Geology, v. 48, p. 43–79, URL <https://doi.org/10.2113/48.1.43>.

Reimchen, T.H.F. (1980): Surficial geology, Dawson Creek, West of the Sixth Meridian, British Columbia; Geological Survey of Canada, Map 1467A, scale 1:250 000, URL <https://doi.org/10.4095/120060>.

Roth, M.P., Verdecchia, A., Harrington, R.M. and Liu, Y. (2020): High-resolution imaging of hydraulic-fracturing-induced earthquake clusters in the Dawson–Septimus area, northeast British Columbia, Canada; Seismological Research Letters, v. 91, p. 2744–2756, URL <https://doi.org/10.1785/0220200086>.

Stott, D.F. (1982): Lower Cretaceous Fort St. John Group and Upper Cretaceous Dunvegan Formation of the foothills and plains of Alberta, British Columbia, and District of Mackenzie and Yukon Territory; Geological Survey of Canada, Bulletin 328, 124 p., URL <https://doi.org/10.4095/119100>.

van Ginkel, J., Ruigrok, E. and Herber, R. (2019): Assessing soil amplifications in Groningen, the Netherlands; First Break, v. 37, p. 33–38.

Worden, C.B., Gerstenberger, M.C., Rhoades, D.A. and Wald, D.J. (2012): Probabilistic relationships between ground-motion parameters and modified Mercalli intensity in California; Bulletin of the Seismological Society of America, v. 102, p. 204–221, URL <https://doi.org/10.1785/0120110156>.